

Research Article

Bench-Scale Flushing Experiments for Remediation of Hg-Contaminated Groundwater

Sung-Wook Jeon

Department of Earth and Environmental Sciences and The Earth and Environmental Science System Research Center, Chonbuk National University, Jeonju-si, Jeollabuk-do 561-756, Republic of Korea

Correspondence should be addressed to Sung-Wook Jeon; sjeon@jbnu.ac.kr

Received 21 July 2016; Accepted 12 October 2016

Academic Editor: Julie J. M. Mesa

Copyright © 2016 Sung-Wook Jeon. This is an open access article distributed under the Creative Commons Attribution License, which permits unrestricted use, distribution, and reproduction in any medium, provided the original work is properly cited.

Bench-scale laboratory column experiments were conducted to determine the desorption characteristics of Hg in the aquifer material from an area of known elevated Hg concentrations in groundwater under flushing conditions. The experimental results showed that columns packed with perched aquifer material (PA) showed flushing of Hg, with the general decline of effluent Hg concentrations over time (from 0.05–0.1 mg/L in the beginning to 0.0001–0.003 mg/L at the end of the experiment). Columns with lower aquifer material (LA) showed nondetectable level of effluent Hg throughout the experiment. Possibility of redissolution/desorption of Hg after static condition (for the duration of 18 days) was tested, showing only slight rebound of Hg concentrations after equilibration. The results suggest that removal of up to 20% of Hg inventory in the sediment could be achievable for the duration of the experiments (about 10 pore volumes). The results also indicate that the treated water from the water treatment plant was more effective compared to deionized water, probably due to complexing agents contained in the treated water.

1. Introduction

Mercury is one of the most toxic contaminants released by gold mining and operation of industrial facilities and elevated mercury concentration down gradient of the mine tailings has been a primary concern for many mining projects [1–5]. Hg contamination in mining impacting aquatic environments is historically due to gold extraction by amalgamation techniques [6]. Extraction with sodium cyanide has also been widely used and caused mercury contamination in the environment [7]. In the extraction, gold is leached from the ores during gold-cyanide process (GCP) [8, 9]. In addition to forming gold complexes, cyanide also coordinates other metals such as iron, zinc, copper, and mercury, forming soluble metal-cyano complexes in leachate solution, causing a serious environmental problem [10].

The fate and transport of mercury in the contaminated systems are controlled by the interaction between aqueous speciation and sediment-water partitioning [11–13]. The aqueous speciation of Hg is strongly affected by chemical conditions such as pH, redox, and concentrations of organic and inorganic ligands [14, 15]. While environmental impact of

mine drainage, which is often acidic and containing elevated levels of mercury, is assessed at some mines, successful remediation measures are not fully implemented [16].

Recent efforts for remediating Hg-contaminated water include methods using zerovalent iron (ZVI) [17–19], elemental Cu and S, granular activated carbon (GAC), attapulgite clay (ATP) [18], and biochars [20]. However, in situ technologies to remediate Hg-contaminated groundwater yet need to be developed. In this regard, only a few studies have been conducted to investigate the controls on Hg mobility and leaching persistence originated from mine tailings [21, 22].

In this study, bench-scale column flushing experiments were conducted to mitigate elevated dissolved mercury concentrations down gradient from the mine tailings at a gold and silver mine. The flushing experiments evaluated whether injected water can flush redissolved/desorbed Hg in the aquifer under the ideal conditions in the laboratory, from which determination can be drawn with regard to the actual remedial performance in the field.

Little is known about the geochemical characteristics of the aquifer matrix at the site with respect to adsorption/desorption properties for contaminants and in particular

mercury in solution. Understanding these characteristics is integral to developing the most efficient remedial strategy and to constraining the estimates for completion of aquifer remediation. The bench-scale laboratory column experiments were conducted to augment the pilot aquifer flushing test to determine the desorption characteristics of Hg in the aquifer material from an area of known elevated Hg concentrations in groundwater. Key objectives of the study were (1) to determine maximum achievable removal of Hg from aquifer solids using potential flushing water, including water sourced from the water treatment plant, which is located downgradient from the tailings, and deionized water and (2) to determine Hg desorption behavior in aquifer solids and to determine the potential for postflushing desorption of Hg from aquifer solids.

The experiments were performed in small columns, measured Hg concentrations overtime, and provided empirical information on the number of pore volumes required for successful flushing. In addition, following initial flushing, columns were permitted to equilibrate and residual Hg concentrations in pore water were measured to evaluate the potential for postflushing desorption and whether this geochemical process could contribute to unacceptable residual Hg concentrations in groundwater. The results will help to define the threshold of reasonably achievable remediation of Hg from the aquifer.

2. Materials and Methods

2.1. Sediments and Source Water. The mining of gold and silver ore at the mine site began in early 1990s. The tailings are dry-filtered and placed in an adjacent mountain slope. Cyanide used in the milling process is discharged with the tailings. Typically, the tailings are disposed with a maximum moisture content of 15 wt.%. Although the tailings have low moisture content, monitoring identified an extensive plume of groundwater contaminated with Hg in the unconfined aquifer. The mercury treatment plant and the planned remedial system site are located approximately 5 km downgradient from the tailings.

Aquifer materials for filling the columns were collected from the drilled cores at the pilot test remedial system site. Three sediment cores were collected at the site and sent to the laboratory. One core represents perched aquifer sediment and was collected from depth of 17.5 to 18.5 m. This depth of the core contains poorly graded sand and gravel with maximum particle size of 60 mm. Particles are subrounded to rounded and have brownish color with black patches. Sediment has some moisture content and is odorless. Two other cores were from the lower aquifer and represent samples from 35 to 36.5 m and from 41 to 42.5 m. The core from depth of 35 to 36.5 m contains soft silty sand and is very wet. The core from depth of 41 to 42.5 m also contains silt to sandy silt with orange mottling and is moist. These two cores were treated essentially as the same material and thus were mixed together during the column packing. For characterization of the sediments, paste pH, particle size distribution, total organic and inorganic carbons, metals, and total sulfur were

analyzed and the results are presented in Table 1. Of note, mercury (Hg) content in sediment samples was 0.196 mg/kg for perched aquifer material and 0.0287 mg/kg for lower aquifer material.

A total of 20 liters of treated water from the water treatment plant at the site were sent to the laboratory. The pH, alkalinity, electrical conductivity (EC), total cyanide, and dissolved metals including mercury were analyzed for the received water, as the results presented in Table 2. Deionized water was also used for the experiments to test the performance in comparison to the treated water.

2.2. Column Setup. A total of six flow-through columns were manufactured and the column experiments were conducted simultaneously. Two columns were packed with the sediment from perched aquifer (PA): one received deionized water (DI) and another received treated water from the treatment plant (TW). Three columns were packed with the sediment from lower aquifer (LA). One column received the treated water, while two other columns received deionized water. The latter two columns (LA-DI1 and LA-DI2) were set up as duplicates to test reproducibility of the experiments. The sixth column contained only silica sand (SS) and received deionized water as the influent. It served as a control column.

For all of the columns, except the control column (SS-DI), approximately 2.5 cm of clean silica sand was layered at the influent and effluent ends of the columns to improve the distribution of flow in the columns and to filter coarse solids out of the effluent. Silica sand was washed with 5% HNO₃ solution overnight and then rinsed with plenty of deionized water until pH is back to normal (>pH 5). The control column was about half filled only with silica sand and thus pore volume was less than other columns. Characteristics of each column are summarized in Table 3.

Each column consisted of a clear acrylic tube, 21.5 cm length and 15 cm internal diameter, and was fitted with end plates. Column dimensions have been selected to optimize the flow rate to allow for a low velocity flow representative of typical field conditions in the aquifer sediments and also to accommodate representative volume of aquifer materials.

Aquifer sediments were retrieved from the cores inside a N₂ glove bag to minimize disturbance of redox conditions in the sediments. The glove bag was fully inflated with N₂ gas and then deflated three times after a core was located inside the bag. Sediments were retrieved under positive pressure of N₂ and thus oxygen intrusion was minimized. After all of the sediments were retrieved from the cores, each of aquifer materials (PA or LA) was mixed by hands to homogenize the sediments as much as possible. This was to ensure that sediments in the columns should have representative samples for each aquifer material. Some large particles such as gravel were excluded from the packing materials.

The retrieved sediments (within the glove bag) were relocated into another glove bag. At this point, the column with ~2.5 cm of silica sand at the bottom was put into the same bag. After that, the outer glove bag was once again purged with N₂ gas three times before column packing started. The sediment was packed into the column over the silica sand

TABLE 1: Characteristics of aquifer materials.

Sample	Perched aquifer (PA)	Lower aquifer (LA)	Detection limit
pH (1:2 soil:water)	4.24	6.35	0.01
Particle size			
% gravel (>2 mm)	8.97	5.78	0.10
% sand (2.00 mm–1.00 mm)	18.3	14.8	0.10
% sand (1.00 mm–0.50 mm)	21.9	18.3	0.10
% sand (0.50 mm–0.25 mm)	11.2	9.76	0.10
% sand (0.25 mm–0.125 mm)	10.7	10.7	0.10
% sand (0.125 mm–0.063 mm)	5.23	6.86	0.10
% silt (0.063 mm–0.0312 mm)	7.17	8.37	0.10
% silt (0.0312 mm–0.004 mm)	10.6	14.8	0.10
% clay (<4 μ m)	6.04	10.7	0.10
Texture	Sandy loam/loamy sand	Sandy loam	
Organic/inorganic carbon			
CaCO ₃ equivalent (%)	<0.80	<0.80	0.80
Inorganic carbon (%)	<0.10	<0.10	0.10
Total carbon (%)	0.1	<0.1	0.1
Total organic carbon (%)	0.10	<0.10	0.10
Metals			
Aluminum (Al) (mg/kg)	31900	54100	50
Antimony (Sb) (mg/kg)	2.48	1.91	0.10
Arsenic (As) (mg/kg)	282	178	0.050
Barium (Ba) (mg/kg)	157	146	0.50
Beryllium (Be) (mg/kg)	0.61	1.34	0.20
Bismuth (Bi) (mg/kg)	<0.20	0.26	0.20
Cadmium (Cd) (mg/kg)	2.07	0.227	0.050
Calcium (Ca) (mg/kg)	1060	2430	50
Chromium (Cr) (mg/kg)	8.77	11.3	0.50
Cobalt (Co) (mg/kg)	50.1	12.8	0.10
Copper (Cu) (mg/kg)	85.9	52.9	0.50
Iron (Fe) (mg/kg)	35000	33900	50
Lead (Pb) (mg/kg)	471	271	0.50
Lithium (Li) (mg/kg)	55.6	25.6	5.0
Magnesium (Mg) (mg/kg)	2610	3010	20
Manganese (Mn) (mg/kg)	7790	2330	1.0
Mercury (Hg) (mg/kg)	0.196	0.0287	0.0050
Molybdenum (Mo) (mg/kg)	2.00	2.16	0.50
Nickel (Ni) (mg/kg)	13.9	8.70	0.50
Phosphorus (P) (mg/kg)	537	509	50
Potassium (K) (mg/kg)	1370	1520	100
Selenium (Se) (mg/kg)	<0.20	<0.20	0.20
Silver (Ag) (mg/kg)	0.38	0.18	0.10
Sodium (Na) (mg/kg)	270	250	100
Strontium (Sr) (mg/kg)	80.1	133	0.50
Sulfur (S), total (mg/kg)	1100	1400	500
Thallium (Tl) (mg/kg)	2.61	0.830	0.050
Tin (Sn) (mg/kg)	<2.0	<2.0	2.0
Titanium (Ti) (mg/kg)	774	787	1.0
Uranium (U) (mg/kg)	0.543	1.18	0.050
Vanadium (V) (mg/kg)	70.6	90.7	0.20
Zinc (Zn) (mg/kg)	358	407	1.0

TABLE 2: Composition of the treated water collected from the water treatment plant.

Parameter	Unit	Concentration	Detection limit
Alkalinity	mg/L as CaCO ₃	14	0.10
pH	—	3.85	0.01
Electrical conductivity (EC)	μS/cm	2950	0.10
Total cyanide	mg/L	0.0231	0.0050
Aluminum (Al)	mg/L	28.2	0.0025
Antimony (Sb)	mg/L	<0.00010	0.00010
Arsenic (As)	mg/L	0.00407	0.00010
Barium (Ba)	mg/L	0.00948	0.00010
Beryllium (Be)	mg/L	0.0147	0.000050
Bismuth (Bi)	mg/L	<0.000025	0.000025
Boron (B)	mg/L	0.917	0.025
Cadmium (Cd)	mg/L	0.00692	0.000025
Calcium (Ca)	mg/L	432	0.10
Chromium (Cr)	mg/L	0.00065	0.00050
Cobalt (Co)	mg/L	0.0764	0.000025
Copper (Cu)	mg/L	0.213	0.00050
Iron (Fe)	mg/L	0.207	0.0050
Lead (Pb)	mg/L	0.000065	0.000025
Lithium (Li)	mg/L	0.712	0.0025
Magnesium (Mg)	mg/L	61.6	0.025
Manganese (Mn)	mg/L	16.6	0.00025
Mercury (Hg)	mg/L	0.000038	0.000010
Molybdenum (Mo)	mg/L	<0.00025	0.00025
Nickel (Ni)	mg/L	0.0430	0.00025
Phosphorus (P)	mg/L	<1.5	1.5
Potassium (K)	mg/L	7.22	0.25
Selenium (Se)	mg/L	0.00054	0.00020
Silicon (Si)	mg/L	47.4	0.25
Silver (Ag)	mg/L	<0.000025	0.000025
Sodium (Na)	mg/L	112	0.050
Strontium (Sr)	mg/L	1.05	0.00025
Thallium (Tl)	mg/L	0.000011	0.000010
Tin (Sn)	mg/L	<0.000050	0.000050
Titanium (Ti)	mg/L	<0.0025	0.0025
Uranium (U)	mg/L	0.00118	0.000010
Vanadium (V)	mg/L	0.00041	0.00025
Zinc (Zn)	mg/L	10.2	0.0025
Zirconium (Zr)	mg/L	<0.00050	0.00050

layer by an increment of about 2.5 cm at each step, after which the column wall was gently tapped by hand to homogenize the sediment inside the column. This step continued until the column was packed leaving only about 2.5 cm at the top. The column packing was completed by filling with silica sand to the remaining portion of the column at the top. Once

column packing was completed, columns were saturated with deionized water before the desired source solutions for each column were introduced. Column weights were measured at each step of the column packing and saturated pore volume (PV) and porosity were calculated from the column weights before and after saturation (Table 3). The column experiments were conducted for a total of 44 days at room temperature.

2.3. Column Operation. Figure 1 shows the schematic of the column experiment. The column experiment was designed so that water enters from the bottom of the column and flows upward discharging from the top of the columns; thus, the bottom of the column is effectively upgradient and the top of the column is downgradient. This was done to ensure consistent and even flow throughout the columns, eliminating the risk of uncontrolled gravity-driven drainage and preferential flow paths.

The nominal residence time in the aquifer layer (excluding ~2.5 cm layer of silica sand at each end of the column) was calculated with the target flow rate of 400 mL/day and the average porosity of 0.3. The actual flow rates in the columns during the experiments were slightly variable, but generally the flow ranged between 350 and 390 mL/day. This corresponded to 0.40–0.45 PV/day, with an exception of the control column. Because of the smaller pore volume, the control column had the flow rates ranging from 0.62 to 0.67 PV/day. With these flow rates, water velocity through the columns was 6.5–7.3 cm/day and residence time was between 2.2 and 2.5 days, indicating that residence time for water in each of the columns is quite similar. By end of the experiment, 9.0–9.5 L of source water had flushed through the columns (Figure 2(a)). With respect to the cumulative PV flushed through the columns, approximately 16 PV flowed through the control column (SS-DI) and 10–11 PV flowed through the other columns (Figure 2(b)).

Following the initial flushing for 16 days, columns were allowed to equilibrate for a period of 18 days without the movement of flushing water through the columns. After the equilibration period, flushing of the columns recommenced and samples were immediately collected from the equilibrated aquifer pore water to determine if postflushing desorption had occurred. This equilibration period is indicated by discontinuities between elapsed days of 16 and 17 in the cumulative effluent volumes and cumulative pore volumes in Figure 2.

2.4. Sample Collection and Analysis. A total of 11 samplings were conducted for each of the columns every two to four days during the total operation period of 44 days. Between elapsed days 16 and 17, pumping was stopped for the duration of 18 days to evaluate if Hg concentration is rebounded due to redissolution/desorption in static conditions; thus, the total elapsed days for the flow-through period, excluding the 18 days of static conditions, were 26 days by the end of the experiment.

For each sampling event, approximately 80 mL of sample was collected from each of the column effluents (40 mL for metals, 15 mL for total cyanide, and 25 mL for pH/

TABLE 3: Column properties.

Column	SS-DI	PA-DI	PA-TW	LA-DI1	LA-DI2	LA-TW
Sediment	Silica sand (SS)	Perched aquifer (PA)	Perched aquifer (PA)	Lower aquifer (LA)	Lower aquifer (LA)	Lower aquifer (LA)
Source water	Deionized water (DI)	Deionized water (DI)	Treated water (TW)	Deionized water (DI)	Deionized water (DI)	Treated water (TW)
Mass of sediment (kg)	3.52	5.35	5.73	5.26	5.43	5.70
Estimated pore water volume (cm ³)	556 ^a	1000	800	835	835	835
Porosity	0.30	0.34	0.27	0.29	0.29	0.29
Elapsed days ^b	26	26	26	26	26	26
Cumulative pore volume (PV) flushed	16.30	10.72	10.63	10.96	10.94	10.51

^aSS-DI was only half filled with silica sand; thus pore volume is less than other columns.

^bBetween elapsed days 16 and 17, pumping was stopped for the duration of 18 days. Thus, the total column operation period was 26 + 18 = 44 days.

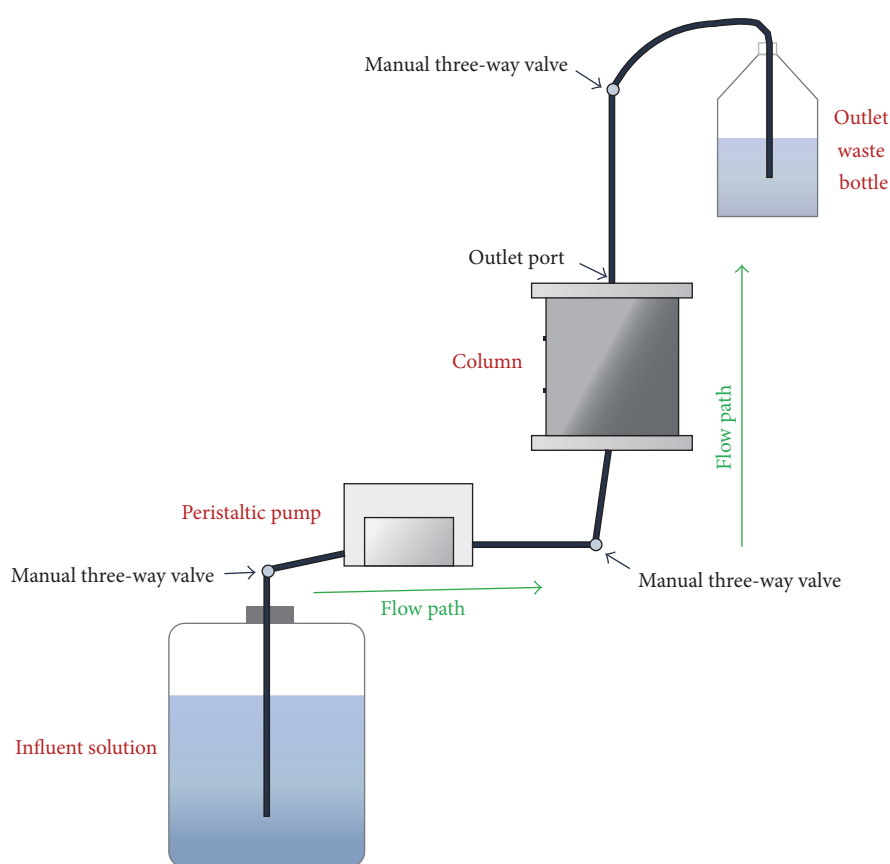


FIGURE 1: Schematic of the column experiment.

alkalinity/EC). To preserve the redox state during sampling, the sampling bottle was purged with nitrogen gas before each of sampling events. Outlet tubing from the sampling bottle was submersed under water to prevent oxygen ingress into the sampling bottle during sampling. Sample was passed through an in-line syringe filter (0.45 μm) so that analyses of dissolved components can be done without interference potentially induced by sampling procedures.

Samples for dissolved metals including Hg were acidified with concentrated, ultrapure nitric acid after filtration.

Samples for total cyanide were prepared by adding 100 μL of 6 N NaOH to a 15 mL of filtered sample. Samples for metals and total cyanide analyses were refrigerated immediately after collection and were analyzed using inductively coupled plasma-mass spectrometry (ICP-MS) and colorimetric analysis (ISO 14403:2002), respectively.

pH, alkalinity, and EC were determined immediately after each sampling event. For pH measurement, a three-point calibration was carried out for the pH meter each time using pH 4.01, 7.00, and 10.01 buffers. Total alkalinity was determined by colorimetric titration with 0.01 M hydrochloric acid. EC

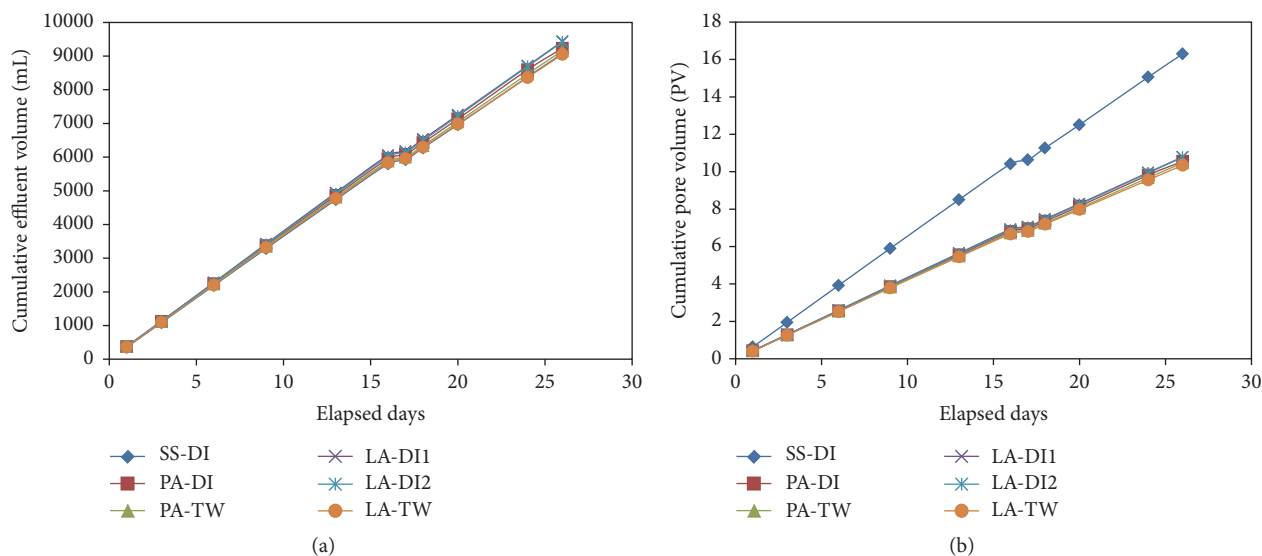


FIGURE 2: (a) Cumulative effluent volume (mL) and (b) cumulative pore volume (PV) for each column.

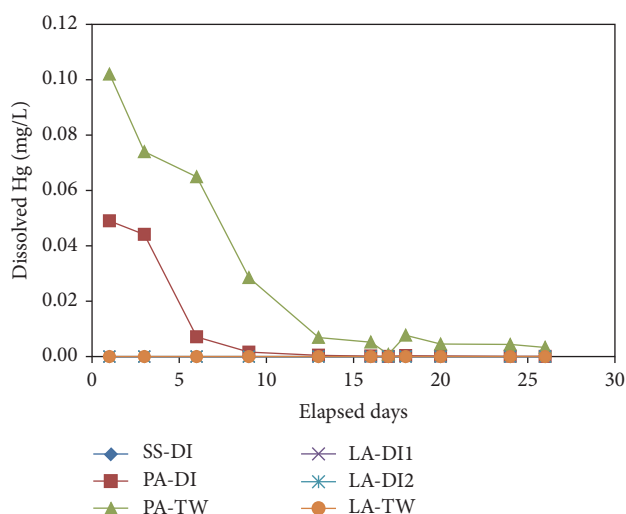


FIGURE 3: Dissolved Hg concentrations measured over time for each column.

was measured by a Thermo Scientific/Orion 5 Star conductivity meter with an Orion 013010MD conductivity cell after calibration with a 1413 $\mu\text{S}/\text{cm}$ conductivity standard solution. Total organic and inorganic carbons, metals, and total sulfur for the sediments were analyzed using gravimetric method [23], ICP-MS, and combustion method (ISO 15178:2000), respectively. Detection limits for the analyses are provided in Tables 1 and 2. Replicate analyses showed little differences.

3. Results and Discussion

3.1. Mercury (Hg). Figure 3 shows the dissolved Hg concentrations for each of column effluents measured over time. Elevated concentrations of dissolved Hg at the effluents were only observed for the columns containing the sediment from

perched aquifer (PA). Column effluents from lower aquifer material (LA) showed nondetectable level of dissolved Hg throughout the column operation the same as the control column (SS-DI). The duplicate columns for LA receiving deionized water (DI) showed the similar behaviors with regard to effluent water chemistry (also for other parameters), suggesting that the sediments were relatively homogeneous between the columns and thus column results are representative at least for the sediments collected in the cores.

The highest dissolved Hg concentration was 0.102 mg/L for PA-TW at day 1 (0.43 PV), while the highest concentration for PA-DI was 0.049 mg/L at day 1 (0.43 PV). The difference in Hg concentrations for the two columns is believed to be due to different complexing abilities of the influent water, primarily represented by total cyanide concentrations (see Figure 4). It is also possible that other complexing agents in the treated water, such as dissolved organic matter (DOM), are responsible for the enhanced Hg recovery. Hg forms strong complexes with organic matter due to its high binding affinity [24, 25]. Also, common complexing ligands, such as chloride and sulfate, can affect the sorption of Hg on the mineral surfaces [26]. Chloride can form aqueous HgCl_2 and Hg_2Cl_2 complexes reducing sorption of Hg. Concentrations of dissolved organic carbon (DOC) and chloride at the effluent water were not measured in this study; however, total organic carbon content in the sediment is higher in the PA than LA (Table 1) and chloride concentration up to 170 mg/L is reported in the downgradient aquifer from the field monitoring data, partially supporting this possibility.

The dissolved Hg concentrations at the effluents continuously decreased to 3.33 $\mu\text{g}/\text{L}$ for PA-TW and 0.079 $\mu\text{g}/\text{L}$ for PA-DI by the end of the experiments. Most of the decline was observed before day 13 (5.58 PV) for PA-TW and day 9 (3.91 PV) for PA-DI. The experimental results indicate that flushing of aquifer by injection of water may achieve decreased level of Hg in the field.

TABLE 4: Hg removal efficiency by flushing.

Column	PA-DI	PA-TW	LA-DI1	LA-DI2	LA-TW
Hg in sediment (mg)	1.048	1.123	0.151	0.156	0.163
Maximum concentration expected in pore water (mg/L)	1.05	1.40	0.18	0.19	0.20
Hg removal by flushing (mg)	0.063	0.22	N/A ^a	N/A ^a	N/A ^a
% Hg removal	6.0	20.3	N/A ^a	N/A ^a	N/A ^a

^aN/A: not applicable.

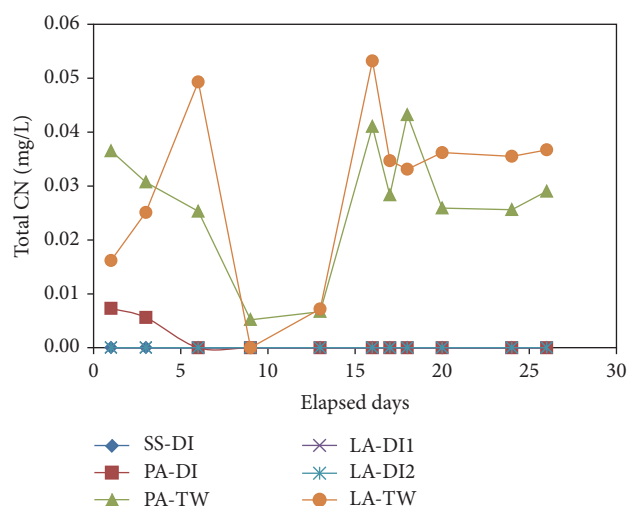


FIGURE 4: Total cyanide (CN) concentrations measured over time for each column.

In the field site, it is reported that almost all of the dissolved mercury in the aquifer pore water is in the form of cyanide complexes and the neutrally charged $\text{Hg}(\text{CN})_2$ complex predominates over other dissolved mercury species at the aquifer pH values. Attenuation of Hg in the main part of the aquifer is only a minor control on dissolved Hg concentrations in the aquifer and the predominance of Hg as a neutrally charged cyanide complex may be responsible for its apparent high mobility in the aquifer. Therefore, the Hg in the sediment cores for this column experiment, which were drilled down gradient of the tailings, can also be present in the form of cyanide complexes.

As explained in Section 2.3, pumping of influent water was stopped for the duration of 18 days between elapsed days 16 and 17, to evaluate if Hg concentration is rebounded due to redissolution/desorption in static conditions. As shown in Figure 3, after the equilibration period, only slight rebound of dissolved Hg concentration was observed only for PA-TW, showing Hg concentration of $7.70 \mu\text{g/L}$ at elapsed day 18 from $0.81 \mu\text{g/L}$ at elapsed day 17 (there is one day of lag time for sampling that has representative effluent water sample from the column). It is not certain whether or not further rebound could be observed over longer period of static condition.

Based on the Hg content in the solid samples (0.196 mg/kg for PA and 0.0287 mg/kg for LA) and sediment masses and pore volumes in each column, the maximum Hg concentrations expected in water, if all of Hg is dissolved into pore

water, were calculated to be $1.05\text{--}1.40 \text{ mg/L}$ for PA and $0.18\text{--}0.20 \text{ mg/L}$ for LA (Table 4). The highest Hg concentration observed in the effluent of PA was 0.102 mg/L , only 7–10% of the maximum concentration expected from complete dissolution. The amounts of water passed through the columns between two adjacent sampling events and the effluent Hg concentrations at each sampling event provide masses of Hg flushed out between the two sampling events. By summing up the masses of Hg flushed out for the entire sampling period, Hg removal by flushing was calculated to be 0.063 mg for PA-DI and 0.227 mg for PA-TW. These values correspond to 6.0 and 20.3% of removal of Hg inventory in the sediments of PA-DI and PA-TW, respectively. The results indicate that flushing of aquifer by injecting water, particularly the treated water, can achieve significant amount of Hg removal from the sediment under the conditions similar to this experiment.

3.2. Total Cyanide (CN). Figure 4 shows the total cyanide (CN) concentrations measured over time for each column. The total CN concentrations at the column effluents were generally low ($0.026\text{--}0.053 \text{ mg/L}$ for PA-TW and LA-TW and nondetectable level ($<0.005 \text{ mg/L}$) for the rest of the columns, except for early times in PA-DI). The effluent total CN concentrations for PA-TW and LA-TW were roughly comparable to the total CN concentration in the treated water (0.0231 mg/L , Table 2). It is also possible that some cyanide was released from the sediments. The lower values for two sampling events at elapsed days 9 and 13 could be experimental artifacts. It appears that the total CN initially present in PA-DI column was flushed out as the deionized source water continued to be supplied to the column.

Cyanide is a strong complexing agent and it may enhance the mobility of many dissolved metals, including Hg, in the tailings pore water. Dissolved mercury cyanide complexes may exist in the forms of $\text{Hg}(\text{CN})_2$, $\text{Hg}(\text{CN})_3^-$, and $\text{Hg}(\text{CN})_4^{2-}$. In the acidic pH conditions in the tailings, anionic mercury cyanide complexes are adsorbed onto clays, iron and aluminum oxides, and oxyhydroxides due to the positive surface charge of these materials [27, 28]. The dissociation of surface cyanide complexes may occur upon geochemical changes [21, 29], which might be the case for the conditions in the flushing column experiments. The pH values of the column effluents ($\text{pH} \sim 4$ for PA and ~ 5 to 6 for LA, Figure 5(a)) were in the range where HCN is the predominant form of free cyanide.

3.3. pH, Alkalinity, and Electrical Conductivity (EC). Figure 5(a) shows the effluent pH values measured over time for

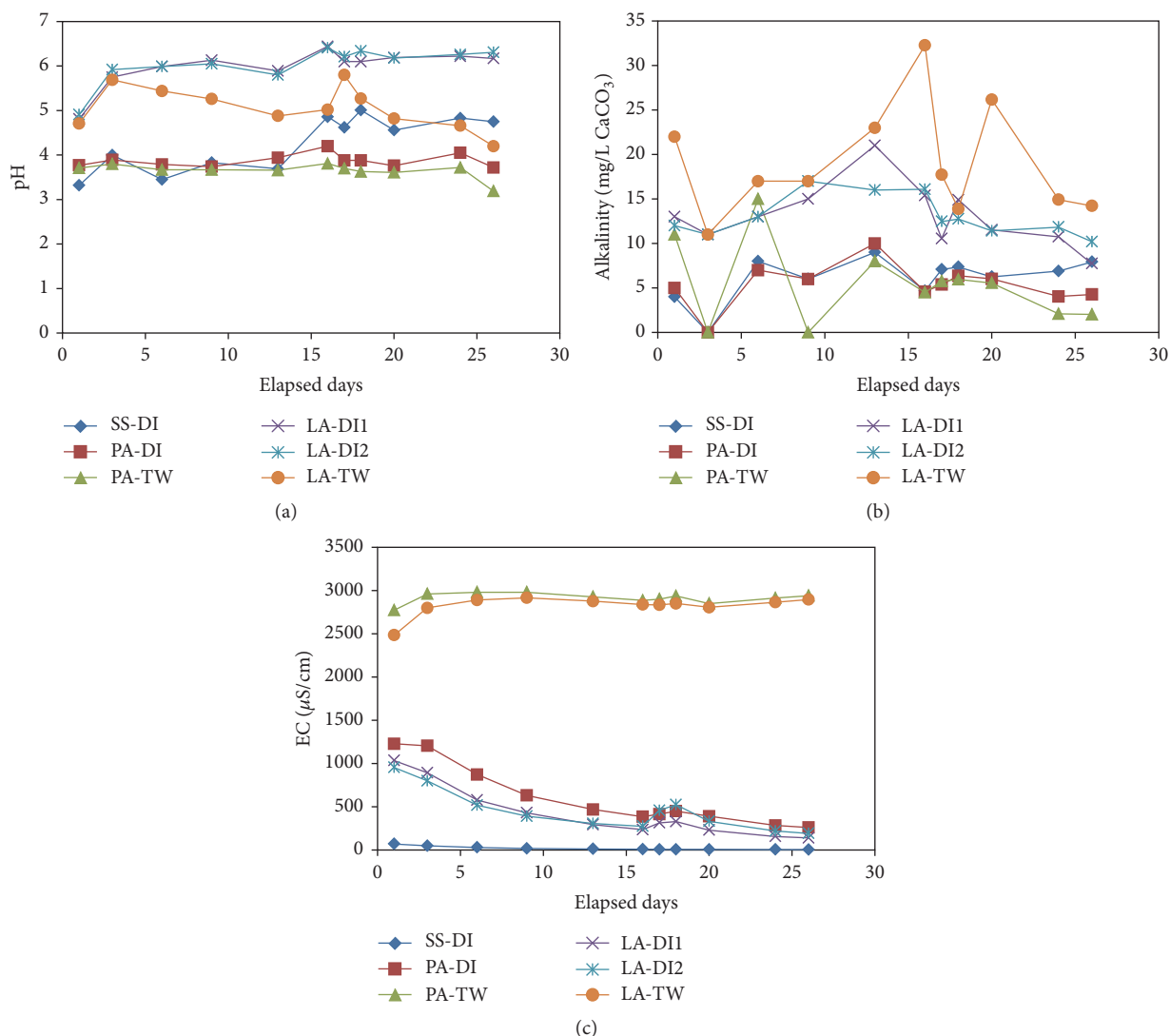


FIGURE 5: (a) pH, (b) alkalinity, and (c) EC measured over time for each column.

each column. Generally, higher pH values for LA columns are observed compared to those for PA columns, which is consistent with the paste pHs for the sediments (4.24 and 6.35 for PA and LA, resp., for 1:2 solid:water, Table 1). This indicates that naturally acidic pH values are present in the perched aquifer due to occurrences of sulfur mineralization in the area. Gradual decline in pH observed for LA-TW could be due to dissolution of aluminosilicate minerals in this column (see Figure 7).

It is not certain why pH for the control column (SS-DI) showed low pH (<4) until day 16. One possible cause is the remnant of acidic pore water that was initially present because of acid washing. As explained in Section 2.2, silica sand was washed with 5% HNO₃ solution overnight and rinsed with deionized water. Although the measured pH for the top water after rinsing was back to normal, some remnant of acidic water might be present in the pore spaces because more silica sand was used for the control column. This potential effect may be minimal for the other columns because only bottom

and top ~2.5 cm ends were filled with silica sand for the other columns, while almost half was filled with silica sand for the control column.

Figure 5(b) shows the total alkalinities measured over time for each column. Alkalinities for PA columns were 4–15 mg/L as CaCO₃, while they were 8–32 mg/L as CaCO₃ for LA columns. For comparison, the influent TW water had alkalinity of 14–17 mg/L as CaCO₃. The higher alkalinity values for LA columns compared to PA columns are probably due to dissolution of carbonate minerals in LA. The Ca contents in the sediments were 1060 and 2430 mg/kg for PA and LA, respectively, and Mg contents were 2610 and 3010 mg/kg for PA and LA, respectively, supporting this explanation. This is consistent with the dissolved Ca and Mg concentrations at the effluents (see Figures 7(a) and 7(b)) and also consistent with the effluent pH values (Figure 5(a)).

The trends of EC (Figure 5(c)) show that dissolved components in the columns receiving deionized water are generally flushed out, while the columns receiving treated

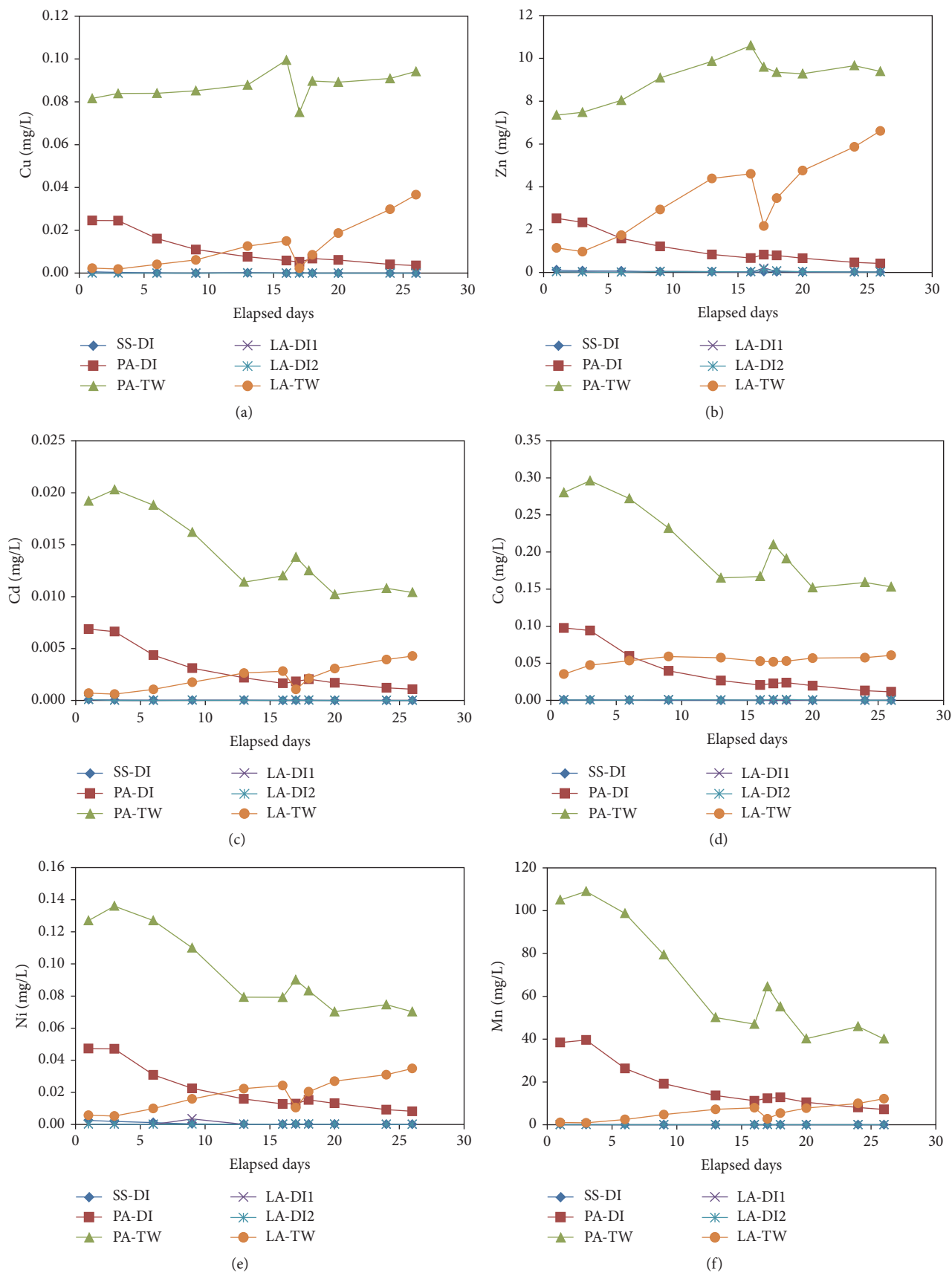


FIGURE 6: Continued.

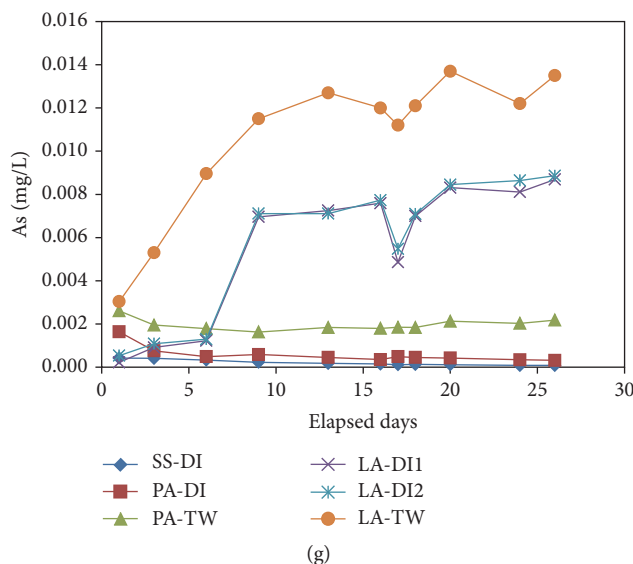


FIGURE 6: (a) Cu, (b) Zn, (c) Cd, (d) Co, (e) Ni, (f) Mn, and (g) As concentrations measured over time for each column.

water show more or less consistent EC over the course of the experiments, primarily due to already high total dissolved solids (TDS) in the treated water.

3.4. Other Metals and Cations. Considering similar complexation behaviors of Hg, Cu, and Zn with cyanide, it was expected that the trends of Cu and Zn concentrations are similar to those of Hg. It was the case for the columns receiving deionized water (Figures 6(a) and 6(b)); however, for the columns receiving the treated water, Cu and Zn concentrations generally increased as the experiment progressed, except for the elapsed days 16 and 17 when the static conditions were tested. This may be partly due to the fact that the sediments contained higher Cu and Zn contents (Cu content of 85.9 and 52.9 mg/kg and Zn content of 358 and 407 mg/kg for PA and LA, resp.) relative to Hg (0.196 mg/kg for PA and 0.0287 mg/kg for LA). While complexation of Cu and Zn with cyanide could explain the elevated Cu and Zn concentrations for PA-TW and LA-TW, the total cyanide concentrations at the effluents were low (0.026–0.053 mg/L for PA-TW and LA-TW), suggesting the presence of other complexing agents in the treated water other than cyanide, similar to the case for Hg.

The trends for Cd, Co, Ni, and Mn (Figures 6(c)–6(f)) were similar to those for Cu and Zn; however, PA-TW showed general decreases in concentrations as the experiment progressed, suggesting flushing of these elements out of the sediments instead of increases in concentrations due to dissolution/desorption or complexation. Dissolved As concentrations at the column effluents were higher for LA than for PA (Figure 6(g)), although the solid sample analyses showed higher value for PA than LA (282 and 178 mg/kg for PA and LA, resp.). Dissolved As, which is not complexed with cyanide, is attenuated due to adsorption onto and coprecipitation with secondary metal oxides and (oxy)hydroxides under neutral or acidic pH conditions [30].

Thus, the release of As in LA columns could be related to desorption of As associated with dissolution of oxides and (oxy)hydroxides that was previously precipitated in this sediment. It may also be caused by reductive dissolution of As-bearing oxyhydroxides such as ferrihydrite [31].

The effluent Ca and Mg concentrations (Figures 7(a) and 7(b)) suggest that dissolution of carbonate minerals could be the source of Ca and Mg in most of the columns, while flushing is predominant in PA-DI. The releases of Al, K, Na, and Si (Figures 7(c)–7(f)) may indicate dissolution of aluminosilicate minerals, such as feldspar, in the sediments. It is shown that the aquifer materials consist primarily of quartz and feldspar, with lesser amounts of clay, mica, and iron oxides and oxyhydroxides. The trends for Al (Figure 7(c)) are different from other elements (K, Na, and Si, Figures 7(d)–7(f)), indicating the precipitation and dissolution of other Al-containing minerals, such as amorphous $\text{Al}(\text{OH})_3$, gibbsite, and alunite, or Al-complexation may also be controlling Al concentrations.

4. Conclusions

The column experiments evaluated removal of Hg from the aquifer sediments using potential flushing waters including the treated water from the water treatment plant and deionized water. The results showed that columns packed with perched aquifer material had flushing of Hg, with the general decline of effluent Hg concentrations over time (from 0.05–0.1 mg/L in the beginning of the experiment to 0.0001–0.003 mg/L at the completion of the experiment). About 5–20% Hg had been flushed out from the sediment during the experiments (about 10 pore volumes), while most of flushing occurred within 5 pore volumes.

The results suggest that flushing of Hg in the aquifer materials by injection of water has the potential to be effective at reducing Hg concentrations in the aquifer. Removal of

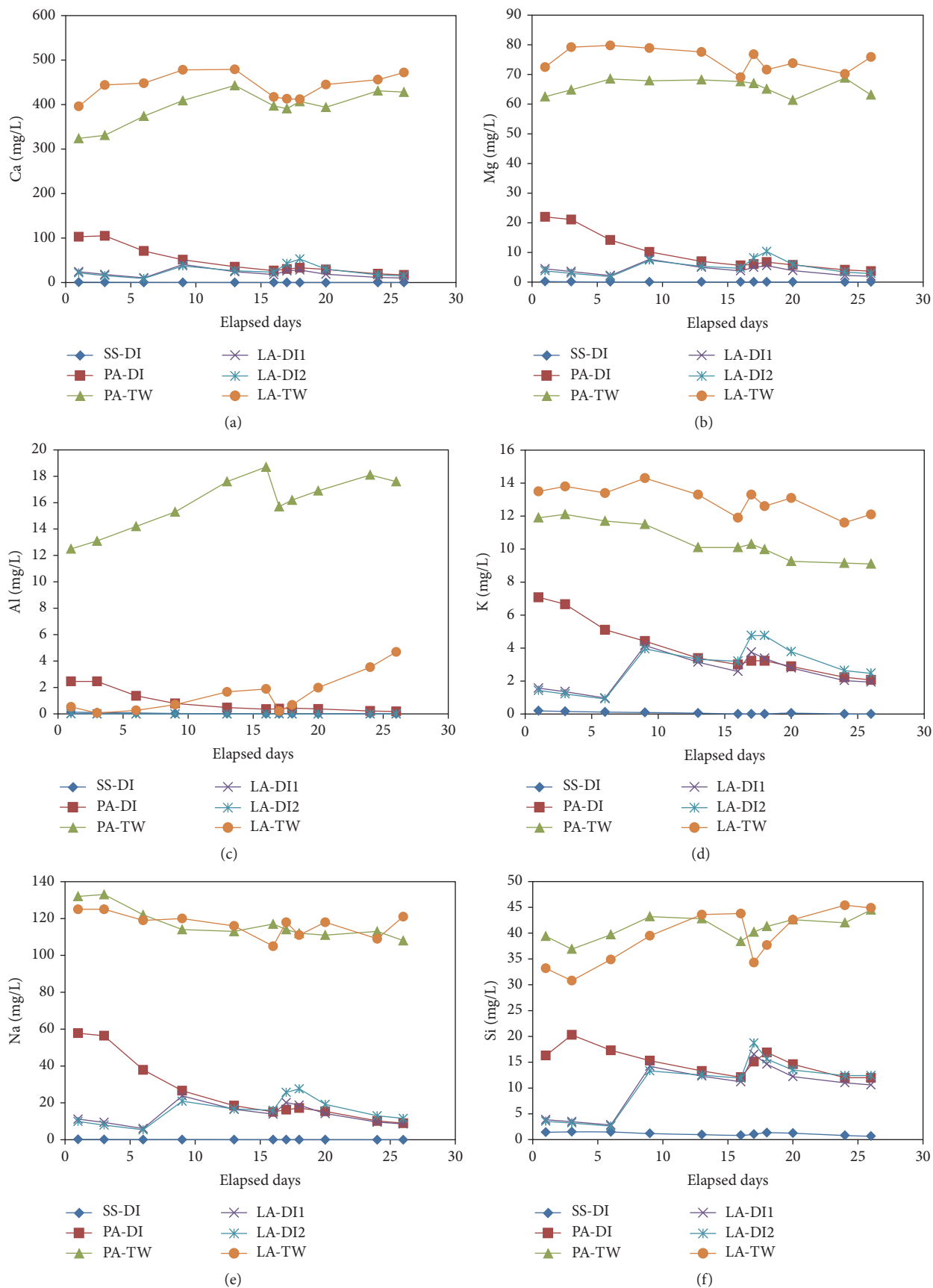


FIGURE 7: (a) Ca, (b) Mg, (c) Al, (d) K, (e) Na, and (f) Si concentrations measured over time for each column.

up to 20% of the Hg inventory in the sediment could be achievable. The results also indicate that the treated water from the water treatment plant is a reasonable flushing solution, probably due to complexing agents contained in the treated water.

It should be noted, however, that the field condition can be different from the experimental conditions. For example, the flow velocity in the column was 6.5–7.3 cm/day, while the groundwater velocity during the injection could be as high as 2 m/day in the field. The difference in contact time may affect dissolved Hg concentrations in the flushed water. Also, the actual field injection may deliver up to 3 pore volumes for a period of 3 months, indicating that extended period of injection may be required to obtain desirable results.

The solid-phase analyses, as well as the results of the column experiments, showed that the perched aquifer contained more Hg compared to lower aquifer and only the perched aquifer showed flushing of Hg out of the sediment. Perched aquifer material has more Hg than lower aquifer material (0.196 mg/kg versus 0.0287 mg/kg). This result indicates heterogeneity of aquifer geochemistry that needs to be considered in the field practice.

Possibility of redissolution/desorption of Hg after static conditions (for the duration of 18 days) was tested, showing only slight rebound of Hg concentrations. However, because of the limited time frame for this study, it is not certain whether or not further rebound could be observed over longer periods of static conditions. Additional testing for longer periods of static conditions could confirm this behavior.

As shown in the experiments, complexation of Hg with complexing agents can enhance removal of Hg by flushing. Testing of water containing added complexing agents, such as ethylenediaminetetraacetic acid (EDTA) and ethylenediamine-*N,N'*-disuccinic acid (EDDS), a biodegradable alternative to EDTA, can be used to evaluate the enhanced removal of Hg by complexation and its potential benefits.

Competing Interests

The author declares that they have no competing interests.

Acknowledgments

Funding for this research was provided by the Basic Science Research Program through the National Research Foundation of Korea (NRF) funded by the Ministry of Education (NRF-2014RIA1A2058040) and by the “R&D Project on Environmental Management of Geologic CO₂ Storage” from the KEITI (Project no. 2014001810003).

References

- [1] W. Salomons, “Environmental impact of metals derived from mining activities: processes, predictions, prevention,” *Journal of Geochemical Exploration*, vol. 52, no. 1–2, pp. 5–23, 1995.
- [2] J. J. Rytuba, “Mercury from mineral deposits and potential environmental impact,” *Environmental Geology*, vol. 43, no. 3, pp. 326–338, 2003.
- [3] United Nations Environmental Programme, “Technical and economical criteria for processing mercury-containing tailings,” Final Report, United Nations Environmental Programme, Division of Technology, Industry, and Economics, 2010.
- [4] S. C. Brooks and G. R. Southworth, “History of mercury use and environmental contamination at the Oak Ridge Y-12 Plant,” *Environmental Pollution*, vol. 159, no. 1, pp. 219–228, 2011.
- [5] D. Watson, C. Miller, B. Lester et al., “Mercury source zone identification using soil vapor sampling and analysis,” *Frontiers of Environmental Science and Engineering*, vol. 9, no. 4, pp. 596–604, 2015.
- [6] J.-C. J. Bonzongo, B. W. Nemer, and W. B. Lyons, “Hydrological controls on water chemistry and mercury biotransformation in a closed river system: the Carson River, Nevada,” *Applied Geochemistry*, vol. 21, no. 11, pp. 1999–2009, 2006.
- [7] M. M. Matlock, B. S. Howerton, M. A. van Aelstyn, F. L. Nordstrom, and D. A. Atwood, “Advanced mercury removal from gold leachate solutions prior to gold and silver extraction: a field study from an active gold mine in Peru,” *Environmental Science and Technology*, vol. 36, no. 7, pp. 1636–1639, 2002.
- [8] A. Tadjeddine and A. Le Rille, “Adsorption of cyanide on gold single crystal investigated by in situ visible-infrared difference frequency generation,” *Electrochimica Acta*, vol. 45, no. 4–5, pp. 601–609, 1999.
- [9] M. A. Rawashdeh-Omary, M. A. Omary, and H. H. Patterson, “Oligomerization of Au(CN)₂⁻ and Ag(CN)₂⁻ ions in solution via ground-state aurophilic and argentophilic bonding,” *Journal of the American Chemical Society*, vol. 122, no. 42, pp. 10371–10380, 2000.
- [10] K. L. Rees and J. S. J. van Deventer, “The role of metal-cyanide species in leaching gold from a copper concentrate,” *Minerals Engineering*, vol. 12, no. 8, pp. 877–892, 1999.
- [11] C. S. Kim, G. E. Brown Jr., and J. J. Rytuba, “Characterization and speciation of mercury-bearing mine wastes using X-ray absorption spectroscopy,” *The Science of the Total Environment*, vol. 261, no. 1–3, pp. 157–168, 2000.
- [12] C. S. Kim, J. J. Rytuba, and G. E. Brown Jr., “Geological and anthropogenic factors influencing mercury speciation in mine wastes: an EXAFS spectroscopy study,” *Applied Geochemistry*, vol. 19, no. 3, pp. 379–393, 2004.
- [13] T. A. Al, M. I. Leybourne, A. C. Maprani et al., “Effects of acid-sulfate weathering and cyanide-containing gold tailings on the transport and fate of mercury and other metals in Gossan Creek: Murray Brook mine, New Brunswick, Canada,” *Applied Geochemistry*, vol. 21, no. 11, pp. 1969–1985, 2006.
- [14] G. A. Gill and K. W. Bruland, “Mercury speciation in surface freshwater systems in California and other areas,” *Environmental Science and Technology*, vol. 24, no. 9, pp. 1392–1400, 1990.
- [15] A. J. Slowey, S. B. Johnson, J. J. Rytuba, and G. E. Brown Jr., “Role of organic acids in promoting colloidal transport of mercury from mine tailings,” *Environmental Science and Technology*, vol. 39, no. 20, pp. 7869–7874, 2005.
- [16] J. J. Rytuba, “Mercury mine drainage and processes that control its environmental impact,” *The Science of the Total Environment*, vol. 260, no. 1–3, pp. 57–71, 2000.
- [17] C. G. Weisener, K. S. Sale, D. J. A. Smyth, and D. W. Blowes, “Field column study using zerovalent iron for mercury removal

- from contaminated groundwater," *Environmental Science and Technology*, vol. 39, no. 16, pp. 6306–6312, 2005.
- [18] B. D. Gibson, C. J. Ptacek, M. B. J. Lindsay, and D. W. Blowes, "Examining mechanisms of groundwater Hg(II) treatment by reactive materials: an EXAFS study," *Environmental Science and Technology*, vol. 45, no. 24, pp. 10415–10421, 2011.
- [19] J. D. Vernon and J.-C. J. Bonzongo, "Volatilization and sorption of dissolved mercury by metallic iron of different particle sizes: implications for treatment of mercury contaminated water effluents," *Journal of Hazardous Materials*, vol. 276, pp. 408–414, 2014.
- [20] P. Liu, C. J. Ptacek, D. W. Blowes, and R. C. Landis, "Mechanisms of mercury removal by biochars produced from different feedstocks determined using X-ray absorption spectroscopy," *Journal of Hazardous Materials*, vol. 308, pp. 233–242, 2016.
- [21] S. A. Shaw, T. A. Al, and K. T. B. MacQuarrie, "Mercury mobility in unsaturated gold mine tailings, Murray Brook mine, New Brunswick, Canada," *Applied Geochemistry*, vol. 21, no. 11, pp. 1986–1998, 2006.
- [22] A. Navarro, E. Cardellach, and M. Corbella, "Mercury mobility in mine waste from Hg-mining areas in Almería, Andalusia (Se Spain)," *Journal of Geochemical Exploration*, vol. 101, no. 3, pp. 236–246, 2009.
- [23] R. H. Loeppert and D. L. Suarez, "Gravimetric method for loss of carbon dioxide," in *Methods of Soil Analysis: Part 3. Chemical Methods*, J. M. Bartels and J. M. Bigham, Eds., Book Series No. 5, ASA and SSSA, Madison, Wis, USA, 3rd edition, 1996.
- [24] C. H. Lamborg, C.-M. Tseng, W. F. Fitzgerald, P. H. Balcom, and C. R. Hammerschmidt, "Determination of the mercury complexation characteristics of dissolved organic matter in natural waters with 'reducible Hg' titrations," *Environmental Science and Technology*, vol. 37, no. 15, pp. 3316–3322, 2003.
- [25] C. L. Miller, L. Liang, and B. Gu, "Competitive ligand exchange reveals time dependant changes in the reactivity of Hg-dissolved organic matter complexes," *Environmental Chemistry*, vol. 9, no. 6, pp. 495–501, 2012.
- [26] C. S. Kim, J. J. Rytuba, and G. E. Brown Jr., "EXAFS study of mercury(II) sorption to Fe- and Al-(hydr)oxides: II. Effects of chloride and sulfate," *Journal of Colloid and Interface Science*, vol. 270, no. 1, pp. 9–20, 2004.
- [27] A. Smith and T. Mudder, *The Chemistry and Treatment of Cyanidation Wastes*, Mining Journal Books Limited, London, UK, 1991.
- [28] T. Rennert and T. Mansfeldt, "Sorption of iron-cyanide complexes in soils," *Soil Science Society of America Journal*, vol. 66, no. 2, pp. 437–444, 2002.
- [29] G. J. Zagury, K. Oudjehani, and L. Deschênes, "Characterization and availability of cyanide in solid mine tailings from gold extraction plants," *Science of the Total Environment*, vol. 320, no. 2-3, pp. 211–224, 2004.
- [30] P. L. Smedley and D. G. Kinniburgh, "A review of the source, behaviour and distribution of arsenic in natural waters," *Applied Geochemistry*, vol. 17, no. 5, pp. 517–568, 2002.
- [31] J. J. Erbs, T. S. Berquó, B. C. Reinsch, G. V. Lowry, S. K. Banerjee, and R. L. Penn, "Reductive dissolution of arsenic-bearing ferrihydrite," *Geochimica et Cosmochimica Acta*, vol. 74, no. 12, pp. 3382–3395, 2010.

